Sirota et al., 2018, Halite focusing and amplification of salt thickness: From the Dead Sea to deep hypersaline basins: Geology, https://doi.org/10.1130/G45339.1.

Data repository 1 - Model Framework

The model developed in this study quantifies the Sirota et al. (2017) conceptual model and described shortly above. The model calculates the amplified annual halite layers at the deep lakefloor based on the abovementioned two halite focusing components.

Under uniform precipitation (Figure A1B), linear precipitation rate will be achieved during the entire level decline (ΔL in m) at a rate of $d = 0.1\Delta L$ (for notation see Table 1) (Lensky et al., 2005). An alternative representation of $\frac{d}{\Delta L}$ is a function of the brine composition (Kiro et al., 2017) that shows variations of $\frac{d}{\Delta L}$ with level decline. Our model calculates amplified annual halite layers in respect to any value of d, because it is a geometry-dependent, relative effect and exists at any brine composition.

The model runs with time steps of one year (because the annual amplification can be calculated precisely for entire year). For convenient, the rate of level decline is also linear and assume to be $\frac{\Delta L}{\Delta t} = 1\frac{m}{year}$, which is close to the current mean rate of Dead Sea decline, but can vary much, usually slower level decline rates, especially under natural conditions . The model is valid for all rates of level decline.

For the first step we calculate the volume of halite available for dissolution at the epilimnetic lakefloor at any time. This halite volume is composed of the annual and multi-year halite components (Figure A1).

Calculation of the annual component (Figure A1B) is done by,

(A1) $h_n = \frac{A_n}{a_n} \cdot d.$

At each yearly step, the annual potential amplification of halite layer by dissolution of the winter halite is by factor of $\frac{A}{a}$, thus is controlled by the bathymetry.

To the total annual component we add the multi-year component. Total annual halite layer, composed of both components is expressed by,

$$(A2)\ H_n = h_n + h_{excess,n}$$

The multi-year component (Figure A1C), h_{excess} calculated by,

$$(A3)\ h_{excess,n} = \frac{\left[(a_{n-1} - a_n) \cdot \sum_{i=1}^{i=n-1} H_i\right]}{a_n}$$

The multi-year focusing component is expected to increase as halite precipitates because increasingly thicker halite units emerge above the thermocline with time.

Using equations 2 and 3, the total deposited annual halite layer at time step t_n is,

$$(A4)\ H_n = h_n + \frac{\left[(a_{n-1} - a_n) \cdot \sum_{i=1}^{i=n-1} H_i\right]}{a_n}$$

The thickness of halite at the hypolimnetic lakefloor (H_T) at any time is,

$$(A5)\ H_T = \sum_{i=1}^{i=n-1} H_i + \frac{\left[(a_{n-1} - a_n) \cdot \sum_{i=1}^{i=n-1} H_i\right]}{a_n}$$

This H_T value yields the maximum amplification potential of halite sequence in case of complete halite dissolution at the epilimnetic lakefloor. A more realistic approach assumes dissolution limits. To the available halite for dissolution on the epilimnetic lakefloor we add two dissolution limits of two origins (expressed by halite volume):

1. Available halite for dissolution (N_h) is the total halite volume on the epilimnetic lakefloor. By definition, this value increases with time because thicker halite layers are elevated to the epilimnion with time.

   $$(A6)\ N_h = a_n \cdot (h_n - d) + H_T \cdot (a_{n-1} - a_n).$$

2. Kinetic limit (N_{kin}) is the ability of the epilimnetic brine to dissolve halite during the interval of undersaturation. Dissolution rates are based on Alkattan et al. (1997) and Stiller et al. (2016). Kinetic limit is calculated in two ways:

(A7) Limit b: $N_{kin} = \frac{C \cdot l_{us} \cdot (A_n - a_n)}{\rho}$

3. Thermodynamic constraint (N_{DD}) is the ability of DD flux to transfer salinity from the upper halite dissolving layer to the lower halite precipitating layer. Calculated thermodynamic limit based on DD flux by Arnon et al. (2016).

(A8) $N_{DD} = \frac{F_{DD} \cdot l_{DD} \cdot a_n}{\rho}$

For each step, after calculating dissolved halite volume under these different limitations, the model uses the lowest value of the three (N_f); this lowest value serves as the limiting factor for the multi-year focusing. Thus, final thickness of each annual halite layer and the total thickness of halite sequence at the hypolimnetic lakefloor is expressed by,

(A9) $H_{nf} = d + (\frac{N_f}{a_n})$

(A10) $H_{Tf} = \sum_{i=1}^{i=n} H_{nf}$

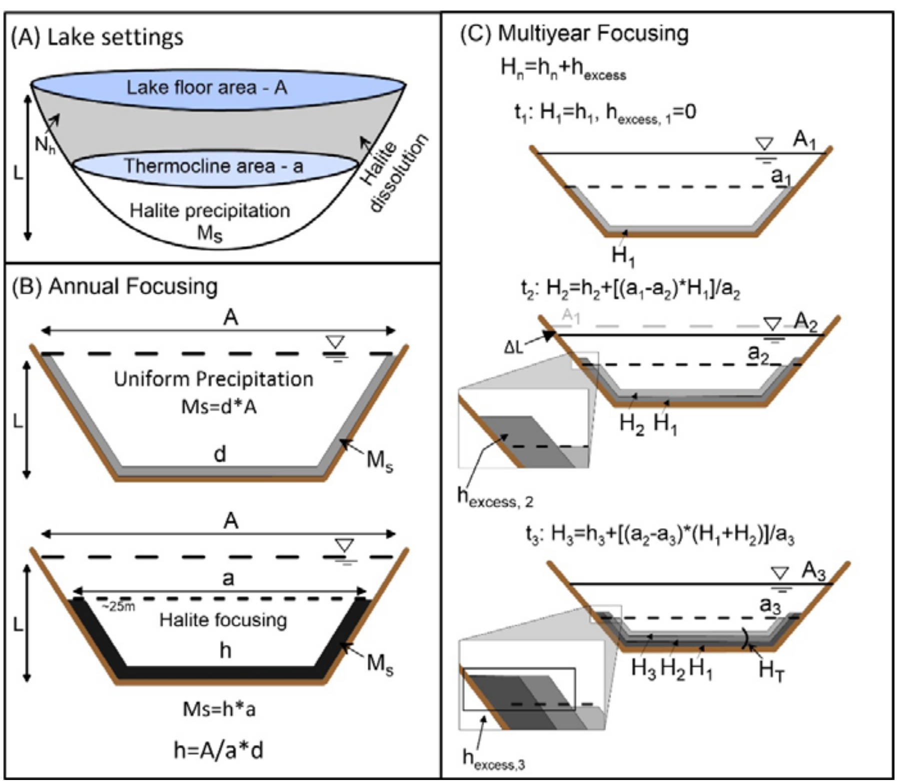

Table 1: Notations list.

Notation	units	
M_s	m^3	Total annual precipitated halite volume.
d	m	Halite layer thickness – uniform precipitation.
h_n	m	Annual halite thickness – annual focusing.
h_{excess}	m	Excess thickness due to inter-annual focusing.
H_n	m	Total annual halite layer thickness.
H_T	m	Halite sequence thickness at the hypolimnetic lakefloor
N_h	m^3	Halite volume at the epilimnetic lakefloor.
N_{kin}	m^3	Annual potential halite dissolution.
F_{DD}	Kg/m^2 d	DD flux.
N_{DD}	m^3	Annual potential salinity transfer by DD flux.
C	Kg/m^2 d	Halite dissolution rate.
l_{us}	d	Duration of undersaturation.
l_{DD}	d	Duration of DD flux.
ρ	2.17 g/cm^3	Halite density
N_f	m^3	Actual annual dissolved halite volume.
H_{nf}	m	Actual annual halite layer thickness.
H_{Tf}	m	Actual halite sequence thickness.

References

Alkattan, M., Oelkers, E.H., Dandurand, J.-L., and Schott, J., 1997, Experimental studies of halite dissolution kinetics, 1 The effect of saturation state and the presence of trace metals: Chemical Geology, v. 137, p. 201–219, doi: 10.1016/S0009-2541(96)00164-7.

Arnon, A., Selker, J.S., and Lensky, N.G., 2016, Thermohaline stratification and double diffusion diapycnal fluxes in the hypersaline Dead Sea: Limnology and Oceanography, v. 61, p. 1214–1231, doi: 10.1002/lno.10285.

Kiro, Y., Goldstein, S.L., Garcia-Veigas, J., Levy, E., Kushnir, Y., Stein, M., and Lazar, B., 2017, Relationships between lake-level changes and water and salt budgets in the Dead Sea during extreme aridities in the Eastern Mediterranean: Earth and Planetary Science Letters, v. 464, p. 211–226, doi: 10.1016/j.epsl.2017.01.043.

Lensky, N.G., Dvorkin, Y., Lyakhovsky, V., Gertman, I., and Gavrieli, I., 2005, Water, salt, and energy balances of the Dead Sea: Water Resources Research, v. 41, p. 1–13, doi: 10.1029/2005WR004084.

Sirota, I., Enzel, Y., and Lensky, N.G., 2017, Temperature seasonality control on modern halite layers in the Dead Sea: In situ observations: Geological Society of America

Bulletin, v. 129, p. 1181–1194, doi: 10.1130/B31661.1.

Stiller, M., Yechieli, Y., and Gavrieli, I., 2016, Rates of halite dissolution in natural brines: Dead Sea solutions as a case study: Chemical Geology, v. 447, p. 161–172, doi: 10.1016/j.chemgeo.2016.10.023.

Data repository 2 – Additional results

The volume of halite that elevated over the thermocline and experienced dissolution increases with time (multiyear component). Thus, it raises the question if these halite units would experience complete dissolution before further level decline and subaerial exposure of the halite. Indeed, rates of halite dissolution are rapid, but would these rates rapid enough to result in complete halite dissolution at the epilimnetic lakefloor?

To examine this question, we apply dissolution limitations upon halite units at the model and calculate the actual thickness of the amplified halite units under these limitations (equations 6-10, DR 1 - model framework).

Considering dissolution limitations, rate of amplification along the sequence decrease, as expected (Figure B1A, dashed curves). Amplification of the sequence increases because of the multi-year focusing component, but rate of amplification restrained because not all the halite focused to the depocenter (Figure B1B).

Dead Sea bathymetry:

The development of the sequence can be divided into two stages. First stage (300-380 m bsl): dissolution does not serve as a limit of the amplification because the focusing components are still small (small A factor). At elevation ~380 m bsl, the annual component increase rapidly and together with the moderate increase of the inter-annual component, become a limit upon the amplification of the sequence. From there, along the course of halite precipitation, amplification ratio stabilizes on 50-60%.

Convex bathymetry:

Under dissolution limits, the accumulation of the sequence divided by us into two stages: First stage: no limiting of focusing by dissolution (complete dissolution at elevation range of 300-440 m bmsl). At this range, the moderate slope results in a large annual focusing from the initiation (initiate with ~20% focusing). Amplification ratio increased moderately until dissolution limits the amplification (at elevation of ~450 m bsl). Second stage: From that elevation, amplification of the sequence limited by dissolution, although the amplification continue. At elevation ~500 m bsl amplification ratio stabilize on ~70%, with a slight decrease towards complete desiccation.

Concave bathymetry:

Under this scenario, the accumulation of the sequence divided by us into two stages: First stage: no limit upon focusing by dissolution (complete dissolution at elevation range of 300-490 m bsl. At that range, the steep slope results in a low dissolution ability of the brine, but also to relatively thin halite units elevated to the epilimnetic lakefloor, thus complete dissolution achieved for 50% of the elevation range. As slope becomes moderate, dissolution ability of the brine increase, but thick halite layers enters the epilimnetic lakefloor, due to the increase in both annual and inter-annual focusing components, thus amplification is limited. Ratio of amplification increased moderately as level declines, reaching ~70% at lowest level.

Sensitivity to basin shape

Halite focusing is a basin-shape dependent; i.e., basin geometry alone affects the magnitude of focusing as level declines. This is shown by modeling focusing using the two ’end member’ synthetic bathymetries: the concave and convex geometries. When limited epilimnetic dissolution is introduced, the hypolimnetic amplification is limited. This limitation results also in limited focusing effect variation between the different basins' shape. The variations in the total focusing effect upon halite sequence under range of basin shapes, 'end-member' bathymetries, are limited up to ~30%.

The results show that Double diffusion flux, through the thermocline that was taking into account as a potential limiting factor did not limit the amplification at any scenario.

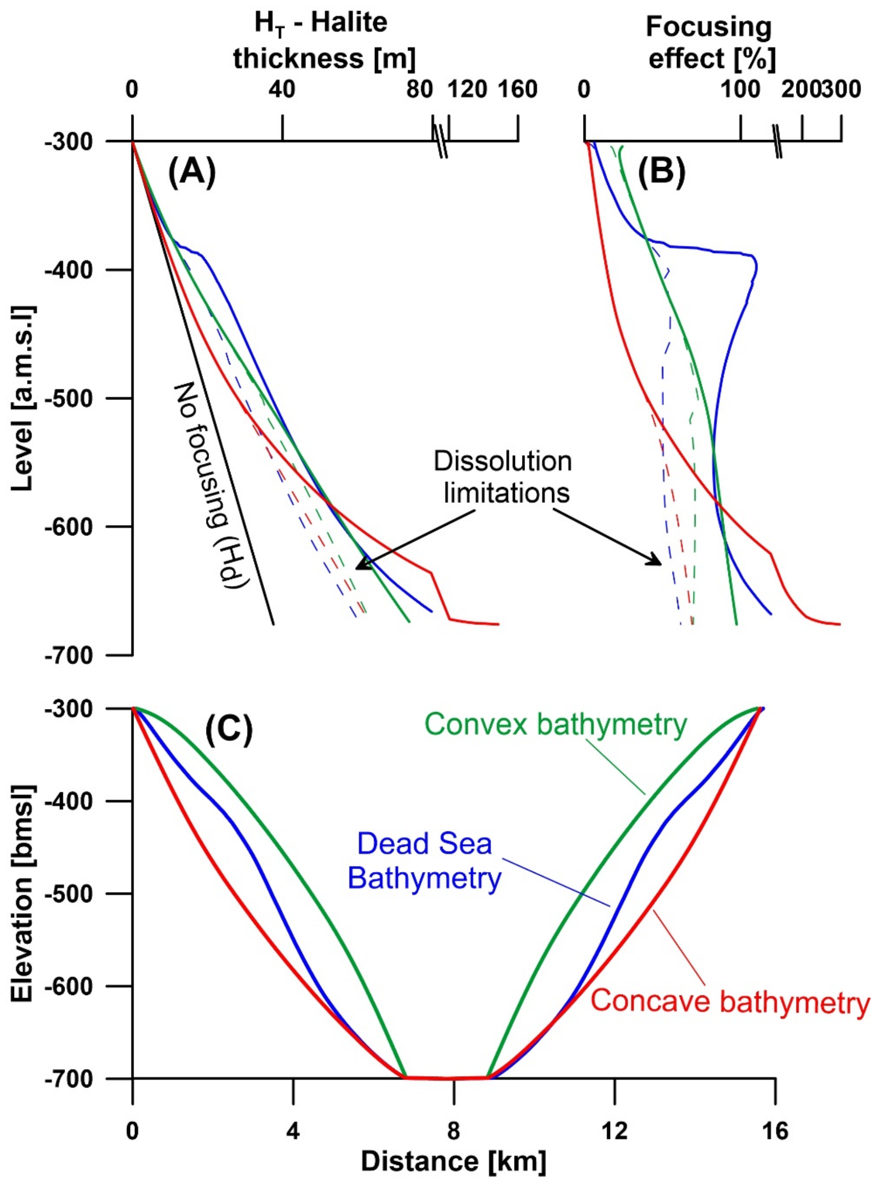

Figure B1: Additional results of halite focusing model, limited by dissolution. (A) Halite accumulation at the depocenter in diverse basins' shapes. The Solid curves are similar as in the results section. The dashed curves display halite accumulation as a response to level decline in case of limited halite focusing by dissolution limitations (see supplementary A - model framework). (B) Focusing effect of the total halite sequence. (C) Transects of the three examined basins' shapes.

DR 3 – thickness variations of the annual layers

The thickness of annual halite layers is associated with the water balance of the waterbody and is used for paleo-Hydroclimatic reconstructions (Manzi et al., 2012; Palchan et al., 2017). The focusing model display significant variations in the thickness of halite layers that amplified due to sub-aquatic halite dissolution. Thus, the shape of the basin strongly influences on the thickness of the annual halite layers.

Figure A displays the three different examined basins. Each basin has a different slope angle along its transect. 'No focusing' scenario consider uniform halite deposition at the entire lakefloor with a fixed deposition rate during level decline, 0.1m of halite deposited for 1m of level decline. For each step of level decline (1m), starting from a level of 300 bsl, the thickness of the related halite layer wad calculated under halite focusing. Figure B displays the focusing effect of the single annual halite layer respect to the 'no focusing' scenario. The annual halite thickness experienced enormous amplification due to halite focusing, up to a potential of 500% amplification. It should be considered that halite at the epilimnetic lakefloor experienced only partial dissolution; thus, the actual amplification is less, but still expected to be significant.

The thickness time series of well-bedded annual halite layers was used for deducing high-resolution climatic cyclicity in the Dead Sea watershed during two last interglacial episodes (Palchan et al., 2017). They observed drastic differences in the mean thickness of annual halite layers between these intervals in the Dead Sea basin. These mean thickness differences can be explained in two ways: either by greater temperature seasonality (colder winters, warmer summers; Sirota et al., 2017) or by focusing under different slope angles during the respective halite intervals. Thus, thicker, deep basin annual halite layers do not always require drier conditions (increased evaporation).

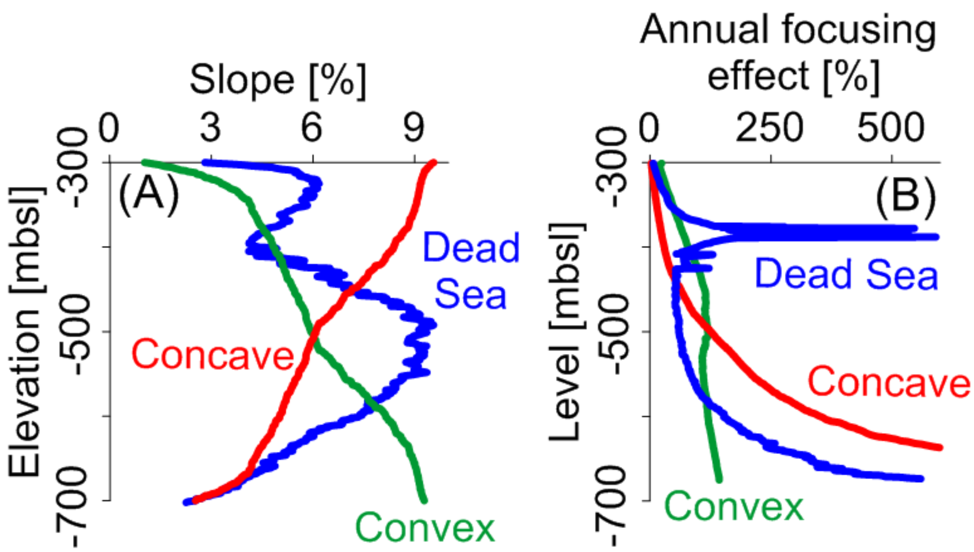

(A) The different examined basins. (B) Focusing effect of a single annual halite layer. The combination of the two focusing components results in major variation of the annual halite layer. Each bathymetry experiences thickness variation along the level decline. In addition, at a specific elevation, halite thickness differs for each bathymetry.

References

Manzi, V., Gennari, R., Lugli, S., Roveri, M., Scafetta, N., and Schreiber, B.C., 2012, High-frequency cyclicity in the Mediterranean Messinian evaporites: Evidence for Solar-Lunar climate forcing: Journal of Sedimentary Research, v. 82, no. 12, p. 991–1005, doi: DOI: 10.2110/jsr.2012.81.

Palchan, D., Neugebauer, I., Amitai, Y., Waldmann, N.D., Markus J., S., Dulski, P., Brauer, A., Stein, M., Erel, Y., and Enzel, Y., 2017, North Atlantic controlled depositional cycles in MIS5e layered sediments from the Dead Sea basin: Quaternary Research, v. 87, no. 1, p. 168–179, doi: 10.1017/qua.2016.10.

Sirota, I., Enzel, Y., and Lensky, N.G., 2017, Temperature seasonality control on modern halite layers in the Dead Sea: In situ observations: Geological Society of America Bulletin, v. 129, no. 9-10, p. 1181–1194, doi: 10.1130/B31661.1.